Soft-Label Caching and Sharpening for Communication-Efficient Federated Distillation

Kitsuya Azuma, *Student Member, IEEE*, Takayuki Nishio, *Senior Member, IEEE*, Yuichi Kitagawa, *Member, IEEE*, Wakako Nakano, *Member, IEEE*, and Takahito Tanimura, *Member, IEEE*

Abstract— Federated Learning (FL) enables collaborative model training across decentralized clients, enhancing privacy by keeping data local. Yet conventional FL, relying on frequent parameter-sharing, suffers from high communication overhead and limited model heterogeneity. Distillation-based FL approaches address these issues by sharing predictions (softlabels) instead, but they often involve redundant transmissions across communication rounds, reducing efficiency. We propose SCARLET, a novel framework integrating synchronized softlabel caching and an enhanced Entropy Reduction Aggregation (Enhanced ERA) mechanism. SCARLET minimizes redundant communication by reusing cached soft-labels, achieving up to 50% reduction in communication costs compared to existing methods while maintaining accuracy. Enhanced ERA can be tuned to adapt to non-IID data variations, ensuring robust aggregation and performance in diverse client scenarios. Experimental evaluations demonstrate that SCARLET consistently outperforms state-of-the-art distillation-based FL methods in terms of accuracy and communication efficiency. The implementation of SCARLET is publicly available at https://github.com/ kitsuyaazuma/SCARLET.

Index Terms—Federated learning, knowledge distillation, non-IID data, communication efficiency.

I. INTRODUCTION

PEDERATED Learning (FL) represents a paradigm shift in distributed machine learning, enabling model training across decentralized clients while preserving data privacy by keeping raw data local. Traditional centralized machine learning typically requires aggregating data at a central server, raising concerns over privacy, security, and compliance. FL mitigates these issues by facilitating collaborative training across clients, such as mobile or edge devices, where only model updates or predictions are communicated with a central server.

Conventional FL methods, such as Federated Averaging (FedAvg) [1], face several fundamental challenges that hinder their scalability and practicality in real-world applications. These challenges include high communication costs from frequent transmission of model parameters, heterogeneous device capabilities and network conditions, convergence difficulties due to non-IID data, and privacy concerns related to the exposure of sensitive information [2]. Addressing these issues is crucial for enhancing the efficiency and robustness of FL systems.

This work has been submitted to the IEEE for possible publication. Copyright may be transferred without notice, after which this version may no longer be accessible.

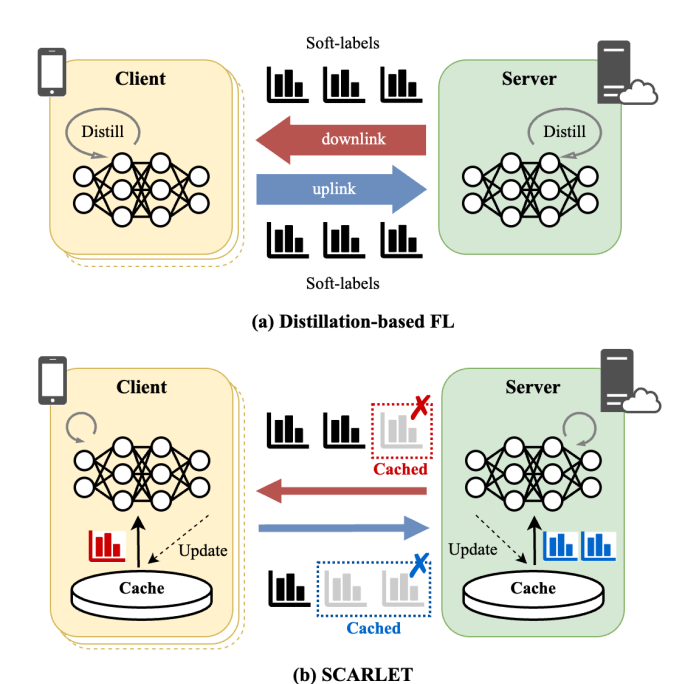


Fig. 1: Conceptual overview of distillation-based FL approaches. (a) Traditional distillation-based FL transmits all soft-labels in each communication round. (b) SCARLET requests soft-labels only for data not present in the server cache and synchronizes cache updates between the server and clients, significantly reducing communication costs.

To mitigate these limitations, recent studies have explored knowledge distillation-based FL approaches, which offer several advantages over conventional parameter-sharing methods. Instead of transmitting full model parameters, these approaches share model predictions (soft-labels), effectively reducing communication overhead [3], [4], [5]. They also provide greater flexibility in model architecture, addressing the systems heterogeneity challenge by allowing clients to operate with heterogeneous models of varying computational capacities [6], [7]. Moreover, since knowledge distillation involves sharing only aggregated or processed outputs rather than raw model updates, it enhances privacy protection by minimizing the risk of exposing sensitive training data through shared gradients [8], [9].

However, existing distillation-based FL methods exhibit significant inefficiencies. Specifically, these methods redundantly

transmit predictions for identical public dataset samples across multiple communication rounds, despite minimal changes in these predictions. This redundancy results in unnecessary communication overhead. Furthermore, current entropy-based aggregation methods used in distillation-based FL (e.g., ERA in [3]) often lack robustness against variations in data heterogeneity across clients, making parameter tuning challenging and degrading performance in diverse non-IID scenarios.

In this work, we introduce **SCARLET** (Semi-supervised federated distillation with global CAching and Reduced soft-Label EnTropy), a novel distillation-based FL approach designed explicitly to resolve these inefficiencies. SCARLET employs synchronized prediction caching between the server and clients to significantly reduce redundant transmissions by reusing cached predictions across rounds, as illustrated in Fig. 1. Additionally, we propose Enhanced Entropy Reduction Aggregation (Enhanced ERA), which dynamically adjusts the aggregation sharpness, offering robust performance and simplified parameter tuning across various levels of client data heterogeneity in non-IID environments.

Our experiments demonstrate that SCARLET consistently outperforms other distillation-based FL methods, achieving target accuracy with reduced communication and faster convergence. This contribution establishes SCARLET as a promising approach for efficient and scalable Federated Learning across heterogeneous client environments.

The key contributions of this paper are summarized as follows:

- Novel Concept of Soft-Label Caching: We propose

 a novel soft-label caching mechanism, which significantly reduces communication overhead by caching predictions for reuse across rounds. To the best of our knowledge, this is the first caching mechanism explicitly designed to eliminate redundant transmission of soft-labels in distillation-based FL, setting a foundation for communication-efficient FL methods.
- **Development of Enhanced ERA:** We propose Enhanced ERA, an improvement over traditional ERA, which prevents overfitting in the global model even in weak non-IID settings by dynamically adjusting aggregation sharpness through a controllable hyperparameter.
- Extensive Comparative Evaluations: We comprehensively evaluate SCARLET against state-of-the-art distillation-based FL methods, demonstrating consistent superiority in accuracy, convergence speed, and communication efficiency across diverse non-IID scenarios.
- Open-Source Implementations for Reproducibility:
 We publicly release the source code for SCARLET
 along with our re-implementations of multiple state-of the-art baseline methods. This facilitates transparent and
 reproducible evaluations and supports future research in
 communication-efficient FL.

The remainder of this paper is organized as follows: Section II reviews related work on parameter-sharing and distillation-based FL methods. Section III describes the SCARLET framework, including the prediction caching mechanism and adaptive aggregation strategies. Section IV presents our experimental evaluation. Section V discusses the limitations of the

proposed method, and Section VI concludes with a summary of findings and future directions.

II. RELATED WORK

A. Federated Learning (FL)

Federated Learning (FL) is a framework for training machine learning models across decentralized clients while preserving data privacy. Since its introduction by [1] with the Federated Averaging (FedAvg) algorithm, FL research has focused on challenges like communication efficiency, non-IID data distributions, and scalability.

Handling heterogeneous data, or non-IID data, where client distributions differ significantly, is a key challenge in FL. Traditional FL methods such as FedAvg are not optimized for these non-IID settings, resulting in slower convergence and reduced accuracy. Various solutions have been proposed, including personalized FL methods like pFedMe [10], which allows client-specific adaptation, and regularization-based approaches such as FedProx [11], which adds a penalty term to local updates to mitigate client drift. SCAFFOLD [12] addresses local model divergence using control variates, and FedNTD [13] employs selective distillation to retain knowledge from "not-true" classes, maintaining a global perspective without extra communication.

Despite these innovations, most methods still rely on parameter sharing, which incurs communication costs. Efficient knowledge transfer remains crucial, especially in non-IID environments.

B. Communication-Efficient FL

Communication efficiency in FL minimizes data transmission between clients and the server, addressing bandwidth and latency concerns. Techniques include quantization, sparsification, and knowledge distillation.

Quantization reduces the bit precision of model updates, thus lowering data size. FedPAQ [14] applies quantization to compressed client updates for efficiency. FedCOMGATE [15] combines quantization with gradient tracking, aligning local and global updates to support non-IID data while reducing communication.

Sparsification transmits only a subset of gradient elements, focusing on key information. Adaptive Gradient Sparsification [16] dynamically adjusts sparsity based on client needs, using a bidirectional top-k approach that retains key gradients to balance communication efficiency and model accuracy.

Knowledge distillation, which shares distilled knowledge (such as output logits) instead of full parameters, allows model heterogeneity by transmitting only essential information. This approach accommodates model heterogeneity among clients by transferring essential output information rather than the model structure itself. Within distillation methods, approaches like FedDF [17] aggregate client outputs on the server, allowing clients to download an updated model without the need to exchange full parameters. Similarly, FedKD [18] reduces communication costs by employing mutual distillation between a global model and a local model while dynamically

compressing exchanged gradients, achieving significant communication savings without sacrificing performance. However, our research focuses on a different class of distillation methods that exclusively exchange model outputs bidirectionally between clients and the server, further enhancing communication efficiency.

C. Distillation-Based FL

Distillation-based FL reduces the communication overhead from parameter exchange by transmitting only model outputs (logits or soft-labels). Unlike traditional knowledge distillation [19], which compresses models, distillation-based FL enables collaborative learning among heterogeneous clients, managing model heterogeneity while reducing communication.

Some studies use public data in distillation. FedMD [20] enables clients with different models to collaborate by sharing logits derived from a labeled public dataset, allowing clients to refine models without sharing raw data. FD [21] reduces communication by aggregating label-wise average logits normalized by a softmax function from clients' private data, while DS-FL [3] improves on FD by using unlabeled public data and introducing Entropy Reduction Aggregation (ERA) to handle high-entropy aggregated soft-labels in non-IID settings.

Recent methods further optimize communication, personalization, and non-IID handling. CFD [4] employs soft-label quantization and delta coding to reduce data transmission, and COMET [22] clusters clients with similar data, sharing only soft-labels for improved personalization. Selective-FD [23] filters ambiguous knowledge through selective sharing, using client-side selectors and a server-side selector to handle out-of-distribution samples and high-entropy predictions.

However, existing distillation-based FL methods suffer from redundant communication, as they do not evaluate how significantly soft-labels are updated in each communication round and whether transmitting these updated labels is truly necessary. This limitation motivates our proposed method, SCARLET, which explicitly addresses such inefficiencies by introducing a soft-label caching mechanism to minimize unnecessary transmissions.

D. FL with Caching Mechanisms

Several studies have proposed FL methods incorporating caching mechanisms. CacheFL [24] employs a caching mechanism that locally stores global models to reduce training time, enabling resource-limited clients to quickly access cached models. FedCache [25] utilizes sample-specific hash mappings and server-side caching to efficiently deliver personalized knowledge without relying on public datasets. FedCache 2.0 [26] replaces logit exchanges with dataset distillation, treating the distilled datasets as a centralized knowledge cache on the server, from which clients download information aligned with their data.

However, these existing caching approaches fundamentally differ from the soft-label caching mechanism proposed in our method, SCARLET. Specifically, SCARLET's caching mechanism explicitly aims to reduce the communication overhead

associated with redundant soft-label transmission in each communication round of distillation-based FL, addressing distinct challenges and objectives compared to previous methods.

III. PROPOSED METHOD

A. Background and Notations

Consider a cross-device FL setting where K clients are participating while communicating with a central server. We assume an N-class classification task. Each client $k \in [K]$ has its classification model \mathbf{w}_k and labeled private dataset \mathcal{B}_k . Each data sample $b \in \mathcal{B}_k$ is a pair (\mathbf{x}, y) where $\mathbf{x} \in \mathbb{R}^d$ is the input and $y \in [N]$ is the class label.

In FedAvg [1], a standard FL method, each client $k \in [K]$ first updates its model \mathbf{w}_k with its private dataset \mathcal{B}_k using stochastic gradient descent (SGD). Then, each client uploads its updated model parameters or gradients to the server. The server aggregates these uploaded parameters to obtain the updated global model \mathbf{w}_q as follows:

$$\mathbf{w}_g = \sum_{k=1}^K \frac{|\mathcal{B}_k|}{\sum_{j=1}^K |\mathcal{B}_j|} \mathbf{w}_k, \tag{1}$$

where $|\cdot|$ denotes the cardinality (size) of a set. Subsequently, the server broadcasts the global model \mathbf{w}_g to all clients. This procedure is repeated for a finite number of communication rounds.

In DS-FL [3], a distillation-based FL method that serves as the baseline for SCARLET, each client and the server exchange soft-labels instead of model parameters. We assume that each client $k \in [K]$ has not only its labeled private dataset \mathcal{B}_k but also the public unlabeled dataset \mathcal{P} . After each client updates its model \mathbf{w}_k as in FedAvg, it generates local soft-labels $z_k^t = \sigma(\mathbf{x}; \mathbf{w}_k)$ for $\mathbf{x} \in \mathcal{P}^t$, where \mathcal{P}^t is unlabeled public dataset used in communication round t. The local soft-labels z_k^t are uploaded from each client to the server, and the server aggregates them to create the global soft-labels \hat{z}^t with ERA as follows:

$$\hat{z}^t = \text{Softmax}\left(\left.\frac{1}{K}\sum_{k=1}^K z_k^t\right| T\right),\tag{2}$$

where $\operatorname{Softmax}(\cdot \mid T)$ denotes the softmax function with temperature T. As the temperature decreases, the entropy of the softmax function's output also decreases. Subsequently, the server broadcast the global soft-label \hat{z}^t to all clients. In the next communication round, the clients first update their local model with the broadcasted soft-labels \hat{z}^{t-1} and the public unlabeled dataset \mathcal{P}^{t-1} as follows:

$$\mathbf{w}_{k}^{t} \leftarrow \mathbf{w}_{k}^{t} - \eta_{\text{dist}} \nabla \phi_{\text{dist}}(\mathcal{P}^{t-1}, \mathbf{w}_{k}^{t}, \hat{z}^{t-1}), \tag{3}$$

where $\eta_{\rm dist}$ is the learning rate and $\phi_{\rm dist}(\cdot, {\bf w}_k^t, \cdot)$ is the loss function in the distillation procedure. The loss function $\phi_{\rm dist}$ is exemplified by the Kullback–Leibler divergence. Along with the clients' local models, the global model ${\bf w}_g^t$ on the server is also updated with the global soft-labels \hat{z}_t and public unlabeled dataset \mathcal{P}^t .

TABLE I: List of Key Notations

Notation	Description
T	Total number of communication rounds
E	Number of local iterations per round
K	Total number of clients
\mathcal{B}_k	Labeled private dataset of client $k \in [K]$
\mathcal{P}	Unlabeled public dataset
\mathcal{P}^t	Unlabeled public dataset used in round $t \in [T]$
\mathcal{I}^t	Indices of \mathcal{P}^t within \mathcal{P}
N	Number of classes for the classification task
\mathbf{w}_k	Classification models of each client $k \in [K]$
\mathbf{w}_g	Classification model of the server
$\sigma(\mathbf{x}; \mathbf{w})$	Soft-labels generated by model \mathbf{w} for input data \mathbf{x}

To avoid ambiguity, we clarify that in this paper, we refer to the outputs shared in distillation-based FL methods as *soft-labels* rather than *logits*. Although the term *logits* is often used in some prior works, such as [3], to refer to the output of the softmax function, it more commonly denotes the unnormalized model output before softmax function. Consequently, we will consistently use the term *soft-labels* to describe the normalized outputs used in the distillation process, aligning with standard terminology in classification tasks.

For clarity of the paper we list the notation used for the paper in Table I. Superscripts indicate the round index, while subscripts denote the client index.

B. SCARLET: System Design and Workflow

SCARLET (Semi-supervised federated distillation with global CAching and Reduced soft-Label EnTropy) is a novel distillation-based FL framework to address inefficiencies observed in existing distillation-based FL methods. SCARLET integrates synchronized soft-label caching and an adaptive aggregation mechanism called Enhanced ERA, significantly enhancing communication efficiency and adaptability to heterogeneous client environments.

Algorithm 1 describes the overall workflow of SCARLET. While the workflow follows that of DS-FL [3], SCARLET introduces two major differences. First, after local training, each client selectively transmits soft-labels only for public dataset samples that are not currently cached on the server, thereby avoiding the redundant transmissions that are typical in previous methods. This caching mechanism, detailed in Section III-C, synchronizes soft-label storage between the server and clients, significantly reducing communication overhead compared to DS-FL, which retransmits soft-labels in every round.

Second, SCARLET introduces a novel aggregation process at the server after collecting soft-labels. We propose Enhanced ERA, an adaptive aggregation strategy that enables robust control over the entropy of aggregated predictions. In contrast to the original ERA used in DS-FL, which often requires careful tuning of the temperature parameter, Enhanced ERA adopts a new parameterization that allows flexible and stable adjustment of label sharpness. This design enhances robustness and stability under varying degrees of data heterogeneity across clients. Enhanced ERA is described in detail in Section III-D.

Algorithm 1 SCARLET

Server Initialization:

Initialize global model \mathbf{w}_g and all client models $\{\mathbf{w}_k\}_{k=1}^K$ Initialize global cache \mathcal{C}_g and all local caches $\{\mathcal{C}_k\}_{k=1}^K$ Set cache duration D

Distribute public dataset \mathcal{P} to all clients $k \in [K]$

```
for t = 1, \dots, T communication rounds do:
```

Server:

Randomly select subset $\mathcal{P}^t \subset \mathcal{P}$ Compute $\mathcal{I}^t_{\text{req}} \leftarrow \{i \in \mathcal{I}^t \mid i \notin \text{dom}(\mathcal{C}_g)\}$ Send $\mathcal{I}^t_{\text{req}}$ to all clients $k \in [K]$ if t > 1 then Send $\gamma^{t-1}, \hat{z}^{t-1}_{\text{req}}, \mathcal{I}^{t-1}$ to all clients $k \in [K]$ end if

Client
$$k \in [K]$$
 (in parallel): $\mathbf{w}_k^{(t,0)} \leftarrow \mathbf{w}_k^{(t-1,E)}$ if $t > 1$ then
$$\hat{z}^{t-1} \leftarrow \text{UPDATELOCALCACHE}($$

$$C_k, \gamma^{t-1}, \hat{z}_{\text{req}}^{t-1}, \mathcal{I}^{t-1})$$

$$\mathbf{\tilde{w}}_k^{(t,0)} \leftarrow \mathbf{w}_k^{(t,0)}$$
 for $i = 1, \cdots, E_{\text{dist}}$ do:
$$\mathbf{\tilde{w}}_k^{(t,i)} \leftarrow \mathbf{\tilde{w}}_k^{(t,i-1)} - \eta_{\text{dist}} \nabla \phi_{\text{dist}}(\mathcal{P}^{t-1}, \mathbf{\tilde{w}}_k^{(t,i-1)}, \hat{z}^{t-1})$$
 end for
$$\mathbf{w}_k^{(t,0)} \leftarrow \mathbf{\tilde{w}}_k^{(t,E_d)}$$
 end if for $j = 1, \cdots, E$ do:
$$\mathbf{w}_k^{(t,j)} \leftarrow \mathbf{w}_k^{(t,j-1)} - \eta \nabla \phi(\mathcal{B}_k, \mathbf{w}_k^{(t,j-1)})$$
 end for
$$\mathcal{P}_k^t \leftarrow \{\mathcal{P}[i] \mid i \in \mathcal{I}_{\text{req}}^t\}$$
 Send soft-labels $z_k^t \leftarrow \sigma(\mathcal{P}_k^t, \mathbf{w}_k^{(t,E)})$ to server

Server: Set
$$\mathbf{w}_g^{(t,0)} \leftarrow \mathbf{w}_g^{(t-1,E)}$$
 Aggregate $\{z_k^t\}_{k \in [K]}$ with $\mathbf{4}$ to get \hat{z}_{req}^t $\hat{z}_{\text{cached}}^t \leftarrow \{\mathcal{C}_g(i) \mid i \in \mathcal{I}^t \setminus \mathcal{I}_{\text{req}}^t\}$ $\hat{z}^t \leftarrow \hat{z}_{\text{req}}^t \cup \hat{z}_{\text{cached}}^t$ for $i = 1, \cdots, E$ do: $\mathbf{w}_g^{(t,i)} \leftarrow \mathbf{w}_g^{(t,i-1)} - \eta_d \nabla \phi_d(\mathcal{P}^t, \mathbf{w}_g^{(t,i-1)}, \hat{z}^t)$ end for $\gamma^t \leftarrow \text{UPDATEGLOBALCACHE}(\mathcal{C}_g, \hat{z}^t, \mathcal{I}^t, t, D)$ end for

Together, the soft-label caching mechanism and Enhanced ERA distinctly position SCARLET as a highly communication-efficient and robust alternative to existing distillation-based FL methods. The subsequent subsections provide detailed descriptions and analysis of these components.

C. Soft-Label Caching in SCARLET

Mechanism Description: The soft-label caching mechanism is introduced in SCARLET to address the communi-

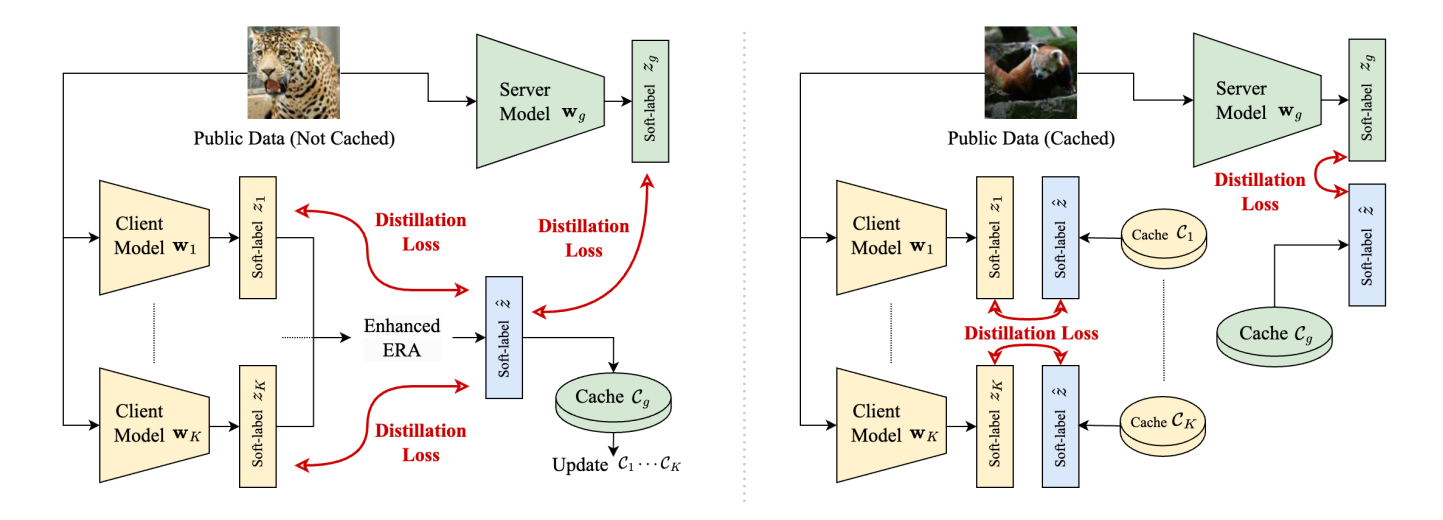


Fig. 2: Illustration of the soft-label caching mechanism in SCARLET. (Left) When public data is not cached, clients transmit their soft-labels to the server, where they are aggregated using Enhanced ERA and stored in the server cache before synchronizing with client caches. (Right) When public data is cached, both the server and clients retrieve soft-labels from their respective caches for knowledge distillation, eliminating the need for additional soft-label communication.

cation inefficiency caused by redundant transmission of softlabels in distillation-based FL methods. Specifically, SCAR-LET reduces communication overhead by caching and reusing soft-labels across communication rounds.

In general, distillation-based FL methods require clients to transmit soft-labels for the same public dataset samples across different rounds, even when the variations in these labels between rounds are minimal. This redundancy arises because local models tend to overfit private datasets during training, resulting in only marginal changes in soft-labels for public data samples. SCARLET addresses this inefficiency by caching and reusing soft-labels for a specified duration, thus reducing redundant transmissions.

The caching process operates on both the server and clients, as illustrated in Fig. 2, ensuring efficient reuse of soft-labels during distillation. The detailed procedure is described in Algorithm 2. At the server side, a global cache \mathcal{C}_g maintains aggregated soft-labels along with the corresponding indices of public dataset samples and their timestamps. At the beginning of each communication round, the server identifies which samples in the selected public subset \mathcal{P}^t are already cached—i.e., those with valid and non-expired entries in \mathcal{C}_g based on a predefined cache duration D. Only the samples that are not cached (either not previously stored or whose entries have expired) are selected for soft-label updates. This selective update mechanism significantly reduces the amount of data transmitted during each round.

Similarly, clients maintain local caches \mathcal{C}_k , which store the soft-labels received from the server. During the distillation process, clients attempt to retrieve soft-labels for public dataset samples from their local caches. For samples that are not cached, the client uses newly received soft-labels from the server and updates its cache accordingly. This dual caching strategy across server and clients minimizes communication overhead while preserving the effectiveness of the distillation

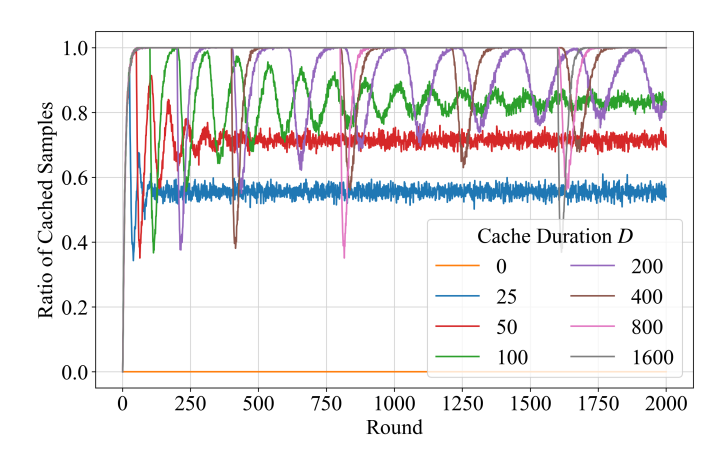


Fig. 3: Simulation of the ratio of cached samples per round as a function of cache duration D. Cached samples are defined as those in \mathcal{P}^t that are found in the local cache and have not expired. The communication cost decreases as the ratio of cached samples increases, since only uncached samples require transmission.

process.

The caching mechanism introduces minimal additional costs compared to the communication overhead it reduces. Each round, the server sends cache synchronization signals, denoted as γ^t in Algorithm 2, to clients. These signals indicate the cache status of public dataset samples and can be represented as integers, resulting in an additional communication cost of $O(|\mathcal{P}^t|)$, where $|\mathcal{P}^t|$ is the number of public dataset samples selected per round. For memory, both the server and clients require $O(|\mathcal{P}| \times N)$ to cache soft-labels, where $|\mathcal{P}|$ is the total size of the public dataset and N is the number of classes. This memory usage is small compared to model sizes in FL and can be further optimized by storing caches on disk if necessary.

Algorithm 2 Soft-Label Caching

```
function UPDATEGLOBALCACHE(C_q, \hat{z}^t, \mathcal{I}^t, t, D)
     Input: Cache C_q, soft-labels \hat{z}^t, indices \mathcal{I}^t,
                  current round t, cache duration D
     Output: Cache signals \gamma^t
     Initialize \gamma^t \leftarrow [\ ]
     for all i, z \in (\mathcal{I}^t, \hat{z}_t) do
           if i \notin dom(\mathcal{C}_q) then
                C_g \leftarrow C_g[i \mapsto (z,t)]
                 Append NEWLY_CACHED to \gamma^t
           else
                 (z_c, t_c) \leftarrow \mathcal{C}_g(i)
                if t - t_c \leq D then
                      Append CACHED to \gamma^t
                else
                      C_g \leftarrow C_g \setminus \{i\}
                      Append EXPIRED to \gamma^t
           end if
     end for
     return \gamma^t
end function
function UPDATELOCALCACHE(C_k, \gamma^{t-1}, \hat{z}_{req}^{t-1}, \mathcal{I}^{t-1})
     Input: Cache C_k, cache signals \gamma^{t-1},
     soft-labels \hat{z}_{\text{req}}^{t-1}, indices \mathcal{I}^{t-1}

Output: Soft-labels \hat{z}^{t-1}
     Initialize \hat{z}^{t-1} \leftarrow []
     Initialize queue Q \leftarrow \hat{z}_{\text{reg}}^{t-1}

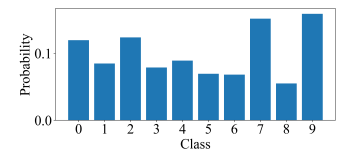
    b treat as FIFO queue

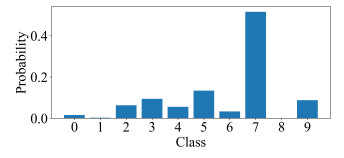
     for all i, z \in (\mathcal{I}^{t-1}, \hat{z}^t) do
           if \gamma^{t-1}[i] is NEWLY_CACHED then
                C_k \leftarrow C_k[i \mapsto Q.\mathsf{pop}()]
                Append C_k(i) to \hat{z}^{t-1}
           else if \gamma^{t-1}[i] is CACHED then
                Append C_k(i) to \hat{z}^{t-1}
           else if \gamma^{t-1}[i] is EXPIRED then
                \mathcal{C}_k \leftarrow \mathcal{C}_k \setminus \{i\}
                 Append Q.pop() to \hat{z}^{t-1}
           end if
     end for
     return \hat{z}^{t-1}
```

Preliminary Evaluation of Sample Cache Ratio: Figure 3 illustrates the relationship between the cache duration D and the proportion of cached samples per round, based on a simulation using the public dataset \mathcal{P} . In each communication round, 10% of the samples in \mathcal{P} were randomly selected to form \mathcal{P}^t , and if a selected sample was already cached, its cached soft-label was reused instead of being updated.

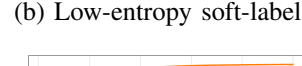
end function

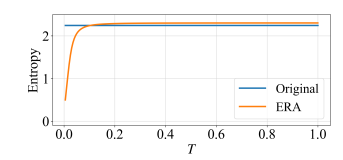
As D increases, a greater number of selected samples remain valid in the cache across rounds, leading to a higher cache hit rate and a corresponding reduction in the need to retransmit soft-labels. However, excessively large values of D reduce the frequency of cache updates, increasing the likelihood of reusing outdated soft-labels—particularly those

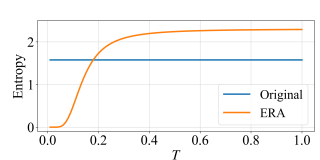




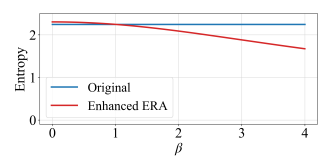
(a) High-entropy soft-label

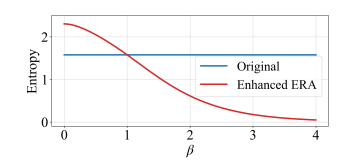






(c) Entropy vs. T using ERA for (a) and (b), shown on the left and right, respectively





(d) Entropy vs. β using Enhanced ERA for (a) and (b), shown on the left and right, respectively

Fig. 4: Comparison of ERA and Enhanced ERA with different parameter settings. Panels (a) and (b) show the original highentropy (low-confidence) and low-entropy (high-confidence) soft-labels, respectively. Panel (c) illustrates how ERA rapidly reduces entropy by decreasing temperature T, particularly for (a) compared to (b). Panel (d) demonstrates how Enhanced ERA provides smoother and more flexible entropy control by varying β , ensuring that $\beta=1$ recovers the original entropy for both (a) and (b).

that significantly deviate from the true labels—which may negatively impact training.

These results demonstrate that the caching module effectively reduces communication overhead while providing a tunable trade-off between the reuse of cached soft-labels and their freshness, controlled via the cache duration parameter D.

The soft-label caching mechanism serves as a versatile and scalable enhancement for FL systems, offering a general-purpose solution to reduce communication costs in distillation-based FL methods. Its design is independent of the underlying aggregation or distillation mechanism, making it easily compatible with existing methods. By integrating this module, other approaches can achieve significant communication efficiency improvements with minimal modifications to their core algorithms.

D. Enhanced ERA in SCARLET

In [3], the ERA method was introduced to adjust aggregated soft-labels, mitigating training stagnation caused by noisy predictions. ERA employs a temperature-adjusted softmax function to systematically reduce the entropy of aggregated client predictions. However, excessively reducing entropy can

negatively impact model accuracy. Furthermore, as demonstrated in our preliminary experiments (Fig. 4(c)), ERA exhibits sensitivity to the temperature T, with optimal values significantly dependent on the initial entropy of the soft-labels. This sensitivity complicates parameter tuning.

To address this limitation, SCARLET proposes **Enhanced ERA**, defined as:

$$\hat{z}_i^t = \frac{\left(\overline{z^t}_i\right)^{\beta}}{\sum_{i=1}^N \left(\overline{z^t}_i\right)^{\beta}},\tag{4}$$

where $\overline{z^t} = \frac{1}{K} \sum_{k=1}^K z_k^t$ represents the averaged local soft-labels, and β controls aggregation sharpness. As β increases beyond 1, Enhanced ERA gradually sharpens the aggregated soft-labels. This sharpening effect is formally described using the concept of *majorization*: the resulting distribution for a larger β is *majorized* by the distribution for a smaller β . This majorization relationship guarantees a monotonic reduction in entropy due to the Schur-concavity of Shannon entropy. For completeness, we provide a proof in the Appendix A.

Enhanced ERA utilizes the *Power Mean* function for aggregating client predictions, resulting in smoother and more consistent entropy control. Figure 4(d) illustrates the relationship between entropy and the hyperparameter β when applying Enhanced ERA. Importantly, when $\beta=1$, Enhanced ERA preserves the original entropy irrespective of the initial entropy level, making it particularly suitable for low-entropy soft-labels that require no entropy reduction. Additionally, Enhanced ERA provides gradual entropy reduction for highentropy soft-labels. While the achievable entropy reduction is more moderate compared to the original ERA (unless extreme β values are employed), the experiments in the following section demonstrate that even this moderate reduction substantially improves model accuracy in distillation-based FL scenarios.

By providing controlled entropy adjustments, Enhanced ERA enables SCARLET to effectively handle different degrees of non-IID data distributions. Specifically, $\beta=1$ maintains the original entropy for weak non-IID scenarios, while setting $\beta>1$ allows gradual sharpening of soft-labels for stronger non-IID conditions. This controlled adjustment simplifies parameter tuning and leads to robust performance across diverse federated learning scenarios. Optimal tuning of β itself, however, remains an open research question and is considered future work. This paper primarily focuses on introducing the fundamental mechanisms of soft-label caching and Enhanced ERA, with detailed discussions regarding hyperparameter tuning provided in Section V.

IV. EXPERIMENTS

A. Experimental Setup

Datasets and Partitioning: SCARLET was evaluated using three combinations of private and public datasets for image classification tasks under heterogeneous data conditions. The detailed dataset configurations are summarized in Table II.

To ensure the robustness of SCARLET in practical scenarios, we deliberately avoided methods that split a single dataset

TABLE II: Dataset configurations and Dirichlet parameters used in SCARLET evaluation.

Private Dataset	Public Dataset	Size Private Public		Dirichlet α
CIFAR-10 CIFAR-100	CIFAR-100 Tiny ImageNet	50,000 50,000	10,000 10,000	0.05, 0.3 0.05
Tiny ImageNet	Caltech-256	100,000	10,000	0.05

TABLE III: Model architectures and input image sizes for each private dataset.

Private Dataset	Model	Input Image Size	
CIFAR-10	ResNet-20	32×32	
CIFAR-100	ResNet-32	32×32	
Tiny ImageNet	ResNet-18	64×64	

into public and private datasets, such as in [3]. Instead, we adopted the approach inspired by [22], where separate datasets with no overlap in image content are used for public and private datasets. This choice reflects real-world conditions, as acquiring a public dataset with identical distributions to private data is often impractical. By utilizing distinct datasets, SCAR-LET aligns more closely with application contexts where such separations are necessary, enhancing the realism and relevance of the evaluation.

The private and public datasets used in our experiments are entirely distinct, with no direct class overlaps. Specifically, CIFAR-10 and CIFAR-100 [27], despite being from the same dataset family, have no overlapping classes. For instance, CIFAR-10 includes categories such as "automobile" and "truck," while CIFAR-100 contains related but separate categories like "bus" and "pickup truck." Similarly, Tiny ImageNet [28] and Caltech-256 [29] cover broad object categories without any direct overlap in image content. While some semantic similarities exist between certain categories across datasets, they do not affect the integrity of the experimental setup.

Data heterogeneity across clients was simulated using a Dirichlet distribution [30] with varying α values. Larger α values approximate IID distributions, while smaller values result in each client holding data from fewer classes. Fig. 5 visualizes the non-IID sample distributions among clients. Smaller α values lead to skewed distributions, where each client primarily holds data from fewer classes. This setup evaluates SCARLET's performance under varying degrees of data heterogeneity and better simulates challenging FL environments.

Models: Table III outlines the model architectures and input image sizes used for each private dataset. For image classification tasks, we tailored ResNet [31] architectures to match each dataset's characteristics. CIFAR-10 and CIFAR-100 both use 32×32 images; however, the increased complexity of CIFAR-100, with its 100 classes, necessitates a deeper ResNet-32 model. For Tiny ImageNet, which has 64×64 images, we used a ResNet-18, which is well suited for intermediate-resolution inputs.

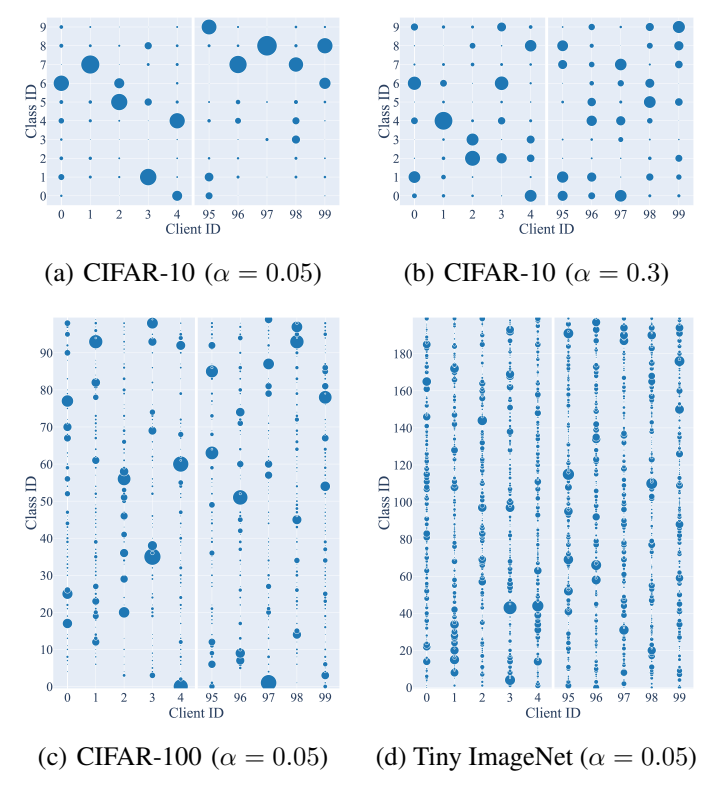


Fig. 5: Visualization of private dataset distributions across clients under different Dirichlet parameters (α). Smaller α values result in more heterogeneous distributions, where clients predominantly hold data from fewer classes.

Although SCARLET and other distillation-based FL methods do not require the server and clients to use the same model architecture, we employed a uniform setup across all entities for simplicity. This consistency helps isolate the effects of SCARLET's communication cost reduction from other factors related to model complexity.

Comparison Methods and Hyperparameter Settings: We evaluated SCARLET's communication efficiency and model accuracy against four state-of-the-art methods: DS-FL [3], CFD [4], COMET [22], and Selective-FD [23].

Unless otherwise mentioned, the following hyperparameter settings were common across all methods. The number of clients was set to 100, each performing 5 local epochs per training round. The learning rate for both local client training and client-server distillation was set to 0.1, following [3]. Each training round utilized 1,000 unlabeled public data samples. For simplicity, we employed stochastic gradient descent (SGD) without momentum or weight decay as the optimizer. The number of communication rounds was determined to ensure sufficient convergence for each private dataset setting: we used 2000 rounds for CIFAR-10 ($\alpha=0.05$), 3000 rounds for CIFAR-10 ($\alpha=0.3$) and CIFAR-100, and 1000 rounds for Tiny ImageNet.

In contrast, method-specific hyperparameters critical to performance, such as the ERA temperature T in DS-FL, were individually optimized through hyperparameter tuning.

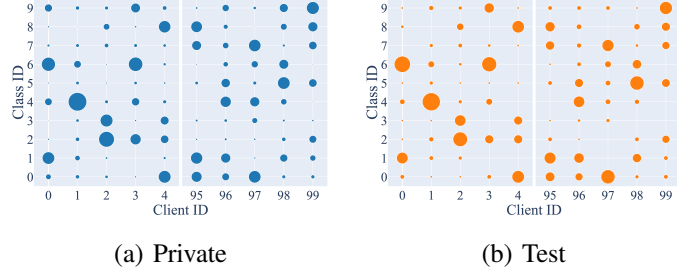


Fig. 6: Comparison of each client's private dataset and test dataset distributions. Both are sampled using the same Dirichlet distribution, ensuring that each client's test set closely matches the class proportions of its private dataset. This setup enables personalized, non-IID evaluation at the client side.

Detailed hyperparameter configurations for each comparative method are provided in Appendix B.

Evaluation Metrics: The evaluation of SCARLET is based on two primary metrics: cumulative communication cost and test accuracy. The cumulative communication cost is defined as the total amount of data exchanged between the server and clients, including soft-labels and other parameters, summed over all clients across communication rounds. We exclude the one-time cost for retrieving the public dataset from this calculation, as it is common to all compared methods and does not affect relative performance.

Test accuracy is measured separately for the server and clients using distinct datasets. For example, when using the train split of CIFAR-10 (50,000 images) as the private dataset, the whole test split (10,000 images) is used for server-side evaluation. The same test split is further partitioned using the same Dirichlet distribution employed for the private dataset, distributing 100 images to each client and enabling client-side evaluation under non-IID conditions (see Fig. 6). This setup ensures that server-side accuracy reflects global performance, while client-side accuracy evaluates personalized performance based on each client's unique data distribution. Notably, client-side accuracy often surpasses server-side accuracy due to the alignment of client-specific test datasets with their training data distributions.

The main analysis presents the relationship between cumulative communication cost and test accuracy through graphs, highlighting both the efficiency and stability of the training process. Additionally, we provide cumulative communication cost values to reach a predefined target accuracy, but emphasize graphical results to better capture the dynamics of learning stability and convergence across methods.

B. Experimental Results

Centralized Learning (Non-FL) Reference Results: Table IV shows the performance obtained by centralized learning, where all clients upload their labeled private data to a central server, and a single global model is trained. These results serve as a reference to illustrate achievable performance levels without the constraints of FL. In this setting, since

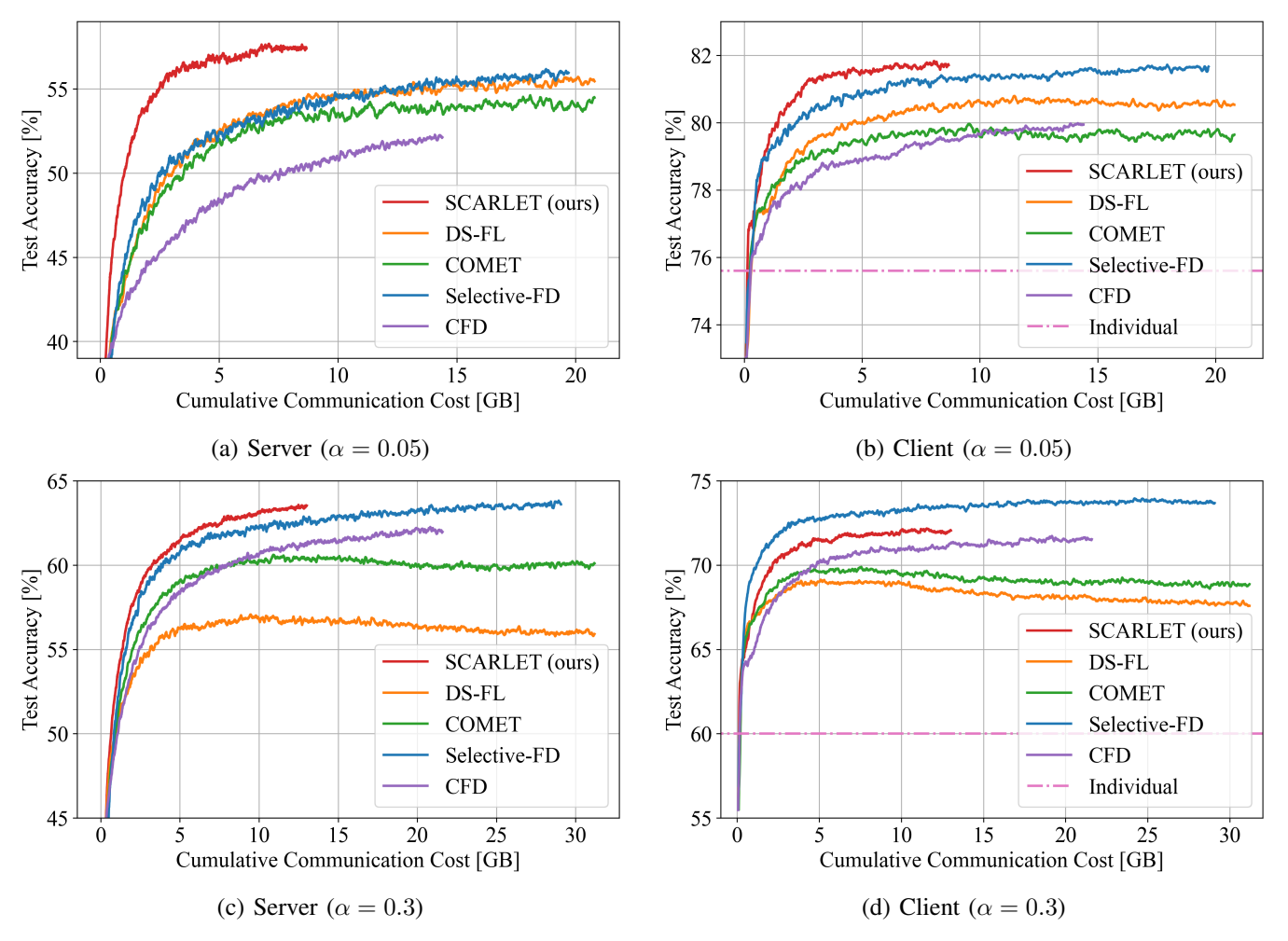


Fig. 7: Test accuracy versus communication cost for SCARLET, DS-FL (baseline), and SOTA methods (CFD, COMET, Selective-FD) on CIFAR-10 under two non-IID conditions: $\alpha = 0.05$ (strong non-IID) and $\alpha = 0.3$ (weaker non-IID).

TABLE IV: Performance of centralized learning on three image datasets.

Dataset	Model	Test Accuracy	
CIFAR-10	ResNet-20	85.4%	
CIFAR-100	ResNet-32	55.5%	
Tiny-ImageNet	ResNet-18	39.5%	

all data is aggregated at a central location, the resulting training data is effectively IID. This often leads to significantly higher accuracy compared to FL conducted under non-IID data conditions.

Note that, unlike the FL experiments which typically employ a higher learning rate, a learning rate of 0.01 is adopted here to ensure stable convergence in the centralized training setting.

Comparative Evaluation: We evaluate SCARLET's communication efficiency and model accuracy by comparing it against four state-of-the-art methods—DS-FL [3], CFD [4], COMET [22], and Selective-FD [23]—as well as an *Individual* baseline that represents isolated client training without collaboration. All results were averaged across three random

seeds, with details of hyperparameter settings for comparative methods provided in Appendix B.

In all experiments, SCARLET employed a soft-label caching mechanism with a cache duration of D=50 and utilized the Enhanced ERA strategy to adapt to non-IID data distributions. The sharpness parameter β in Enhanced ERA was tuned to reflect the degree of data heterogeneity. For CIFAR-10, β was set to 2.0 under strongly non-IID conditions ($\alpha=0.05$) and 1.0 under less heterogeneous conditions ($\alpha=0.3$). For CIFAR-100 and Tiny ImageNet, $\beta=1.25$ yielded optimal results. A more detailed evaluation of the effects of varying α and β is provided in the next section.

Fig. 7 presents the relationship between server-side and client-side test accuracy and cumulative communication cost on CIFAR-10 under strong and moderate non-IID settings. SCARLET outperformed other methods under strongly non-IID conditions ($\alpha=0.05$), achieving approximately 2% higher server-side accuracy while reducing communication costs by over 50%. On the client side, SCARLET matched the peak accuracy of Selective-FD but with similar communication savings. This highlights the effectiveness of SCARLET's caching mechanism and adaptive aggregation in mitigating challenges posed by heterogeneous data distributions.

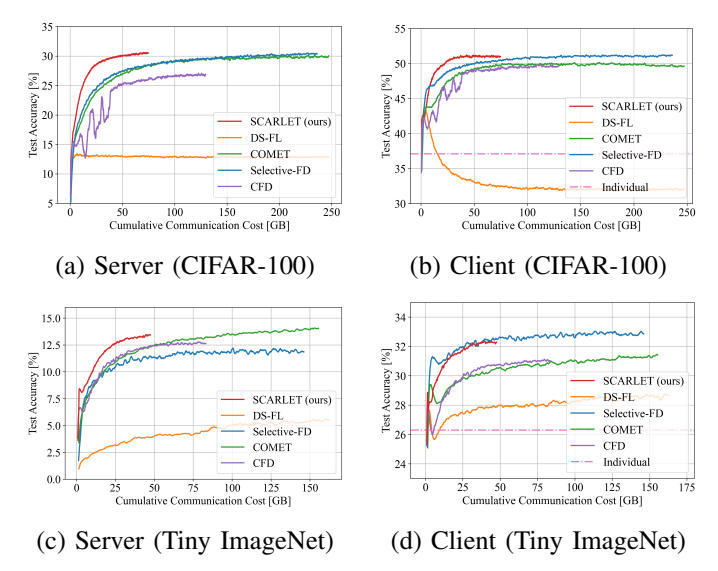


Fig. 8: Test accuracy versus communication cost results on CIFAR-100 and Tiny ImageNet for SCARLET and SOTA methods (DSFL, CFD, COMET, Selective-FD). These results are still under investigation.

Under less severe non-IID conditions ($\alpha = 0.3$), SCAR-LET maintained server-side accuracy comparable to the bestperforming method, Selective-FD, while achieving over 50% lower communication cost. However, Selective-FD demonstrated superior client-side convergence speed and final accuracy, underscoring its strength in personalized learning scenarios. In contrast, DS-FL struggled to achieve high accuracy under these conditions, regardless of how the temperature T in its ERA mechanism was tuned. This limitation can be traced to the presence of aggregated soft-labels with inherently low entropy. When T is reduced excessively, these low-entropy soft-labels approach a one-hot representation, diminishing the effectiveness of the distillation process. Conversely, increasing T too much causes a sudden spike in entropy for certain soft-labels, exacerbating inconsistencies in entropy reduction across public datasets. These issues result in both lower accuracy and performance degradation over time, likely due to overfitting.

SCARLET's Enhanced ERA mechanism, on the other hand, addresses these challenges by enabling consistent and controlled entropy reduction. By dynamically adjusting the sharpness parameter β , SCARLET prevents the pitfalls of overly sharp or overly smooth distributions. For less severe non-IID conditions, β is set to 1.0, effectively simplifying aggregation to straightforward averaging, which is sufficient under such scenarios. This adaptability allows SCARLET to achieve stable and high accuracy, while preserving its hallmark communication efficiency and maintaining compatibility across a wide range of FL scenarios.

Fig. 8 presents the results for CIFAR-100 and Tiny ImageNet, demonstrating the scalability and robustness of SCAR-LET. The soft-label caching mechanism and Enhanced ERA consistently achieved high communication efficiency and competitive accuracy across datasets with more complex label

distributions and greater heterogeneity.

In summary, SCARLET demonstrates robust performance in a variety of challenging FL scenarios. Its integration of the soft-label caching mechanism and Enhanced ERA mechanism not only reduces communication costs significantly but also sustains high model accuracy. While Selective-FD retains advantages in specific client-side settings, SCARLET's adaptability and modular design open pathways for hybrid solutions that leverage the strengths of both approaches. Results on CIFAR-100 and Tiny ImageNet further reinforce SCARLET's potential as a scalable, communication-efficient framework for diverse FL environments.

Effectiveness of the Soft-Label Caching Mechanism in Other SOTA Methods: The soft-label caching mechanism, a core component of SCARLET, is designed to alleviate communication inefficiencies in distillation-based FL. Since such inefficiencies are not specific to SCARLET, the mechanism can also be applied to other SOTA methods to improve their communication efficiency. To evaluate its broader impact, we integrated the caching mechanism into three representative FL methods: CFD, COMET, and Selective-FD. DS-FL was excluded from this evaluation, as it becomes conceptually similar to SCARLET when caching is introduced. For all methods, we used a conservative cache duration of D=25 to balance communication reduction with the risk of overfitting to stale predictions.

Fig. 9 presents the server-side and client-side test accuracy versus cumulative communication cost for each method with the soft-label caching mechanism applied. The results show that incorporating the caching mechanism reduced server-side communication costs by approximately 50% across all three methods, without substantial loss in target model accuracy. Notably, CFD and Selective-FD maintained accuracy levels comparable to their original implementations, indicating that the mechanism imposes minimal performance overhead. On the client side, although communication reductions were less dramatic due to the quicker convergence of personalized models, notable gains were still observed. Selective-FD, in particular, preserved strong personalized accuracy while benefiting from improved communication efficiency. COMET showed slight accuracy degradation in later training rounds, a trend also reflected in its server-side performance.

These findings demonstrate the generalizability and effectiveness of the soft-label caching mechanism. Its seamless integration into a variety of distillation-based FL methods—including CFD, COMET, and Selective-FD—highlights its potential as a practical, drop-in component for enhancing communication efficiency. By incorporating this mechanism, existing FL frameworks can significantly reduce communication overhead while maintaining strong global and personalized model performance, thereby contributing to the scalability and practicality of FL systems.

Ablation Study of Cache Duration: The cache duration D, a key parameter in our soft-label caching mechanism, significantly influences both communication cost and accuracy

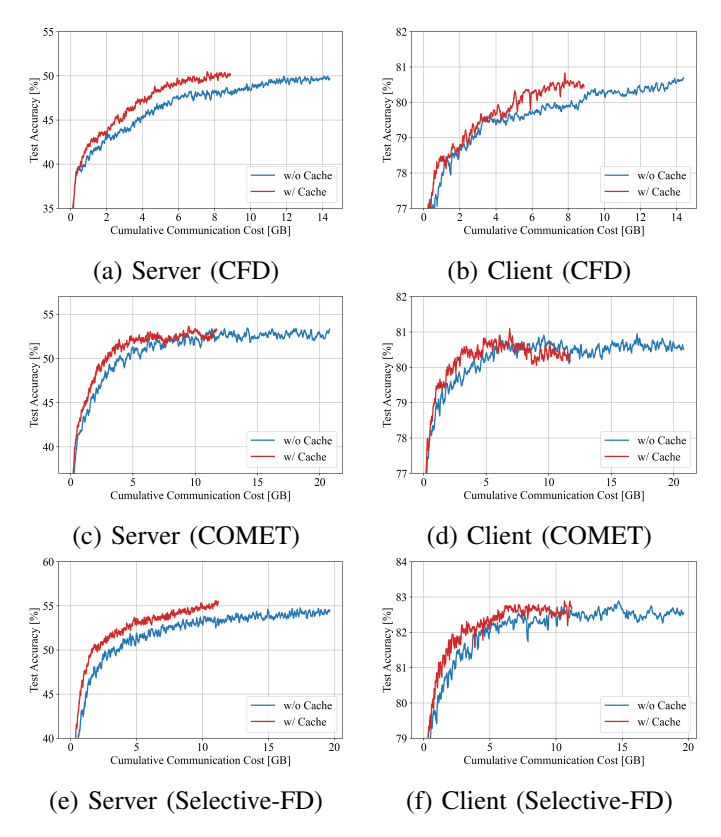


Fig. 9: Impact of the soft-label cache mechanism integration on test accuracy and communication cost for SCARLET applied to CFD, COMET, and Selective-FD. Plots for both server and client sides demonstrate significant communication cost reductions without substantial accuracy degradation.

in SCARLET. We performed a detailed analysis using CIFAR-10 under a Dirichlet distribution with $\alpha=0.05$, as results with other α values showed similar trends and are therefore omitted for brevity.

The results in Fig. 10 demonstrate that increasing D reduces communication costs for both the server and clients, but it also introduces trade-offs in accuracy. On the server side, D=800 makes the system heavily reliant on cached softlabels (see Fig. 3), causing accuracy degradation. Notably, accuracy shows stepwise improvements at multiples of the cache duration, such as rounds 800 and 1600, when the cache is fully refreshed and stale predictions are replaced.

On the client side, D=200 emerges as an optimal duration, achieving higher accuracy than both shorter and longer durations. As shown in Fig. 11, additional analysis with finer values of D highlights that accuracy consistently improves as D approaches 200. This balance allows for stable learning periods without frequent soft-label exchanges, enabling efficient utilization of cached predictions and minimizing the risk of overfitting to stale labels.

These findings highlight the trade-off between communication cost savings and accuracy. While longer cache durations like D=800 reduce communication costs, they risk accuracy drops due to reliance on outdated cached labels, with improvements only at periodic refresh intervals. Durations

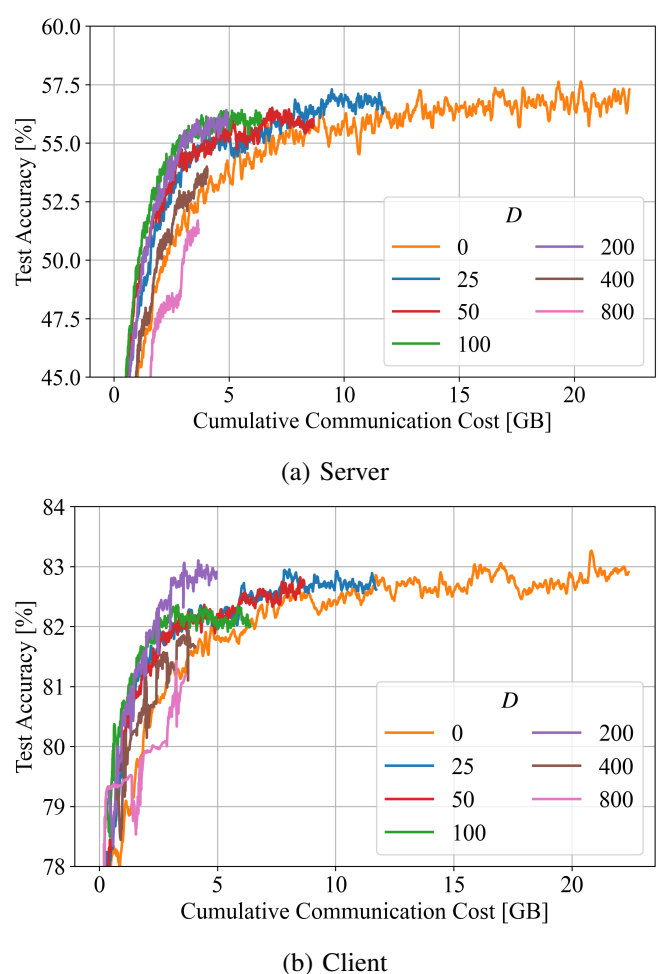


Fig. 10: Impact of cache duration D on test accuracy for SCARLET on CIFAR-10 under a Dirichlet distribution with $\alpha=0.05$. Increasing D significantly reduces communication costs for both the server and clients.

around D=200 offer a practical balance, enabling stable learning periods without frequent soft-label exchanges and minimizing overfitting to cached predictions. As shown in Fig. 3, such durations can often be identified through simple simulations. In cases where determining an optimal duration is challenging, smaller values of D can still provide substantial communication cost reductions with only modest impacts on accuracy. This flexibility makes cache duration a valuable parameter for tuning communication efficiency in FL systems.

Ablation Study of Enhanced ERA: To evaluate the impact of the aggregation sharpness parameter β in the Enhanced ERA mechanism, we conducted experiments on CIFAR-10 under both strong ($\alpha=0.05$) and weak ($\alpha=0.3$) non-IID conditions. A fixed cache duration of D=50 was used in all experiments, and the results are presented in Fig. 12.

For strong non-IID scenarios ($\alpha=0.05$), increasing β values (e.g., $\beta>2.0$) significantly improved server-side convergence, reducing the communication costs needed to reach a target accuracy. This acceleration is attributed to the sharper aggregation of client predictions, which mitigates the

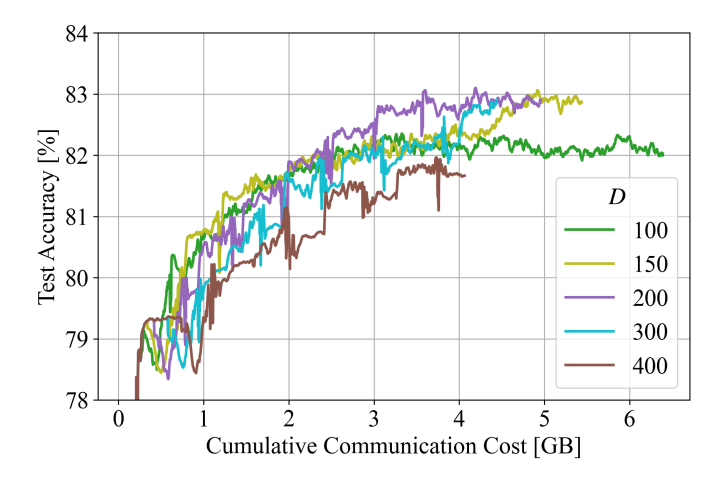


Fig. 11: Additional analysis of finer cache duration values for SCARLET on CIFAR-10 under a Dirichlet distribution with $\alpha=0.05$. The results confirm D=200 as an optimal duration, balancing communication efficiency and accuracy.

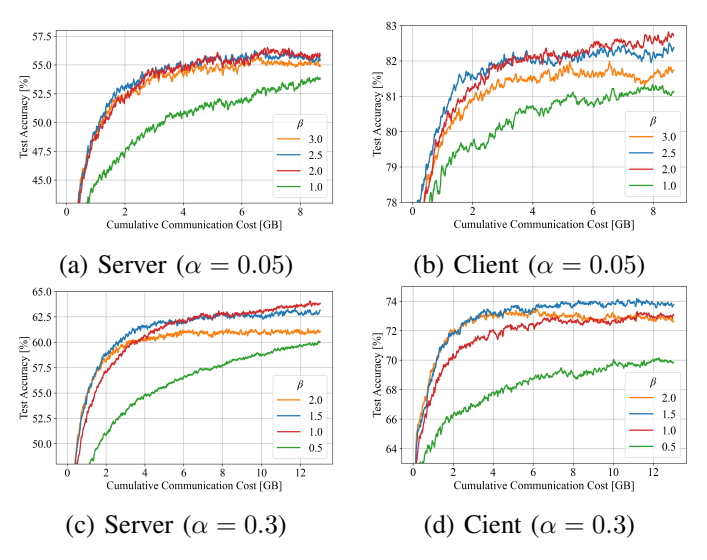


Fig. 12: Impact of aggregation sharpness parameter β in Enhanced ERA on test accuracy for SCARLET on CIFAR-10 under Dirichlet distributions with $\alpha=0.05$ (strong non-IID) and $\alpha=0.3$ (weak non-IID). Varying β demonstrates distinct effects on server-side and client-side accuracy, highlighting the importance of proper tuning.

smoothing effects of locally biased soft-labels. However, on the client side, excessively high β values caused accuracy stagnation in later rounds. This degradation likely results from over-sharpened labels introducing biases during local training, thus limiting the generalization of client-specific models.

For weak non-IID conditions ($\alpha=0.3$), $\beta=1.0$ preserved steady server-side accuracy across all communication rounds, avoiding the risks associated with over-sharpening or oversmoothing. On the client side, $\beta=1.5$ yielded the highest accuracy, striking a balance between effective aggregation and model generalization. Larger β values led to performance degradation, suggesting that less aggressive sharpening is

preferable in scenarios with lower heterogeneity.

These results highlight the necessity of tailoring the value of β to the degree of non-IID-ness in client data distributions. For weakly non-IID or near-IID conditions, smaller β values (e.g., $\beta \approx 1.0$) are sufficient to maintain stable performance while preventing overfitting. Conversely, in strongly non-IID scenarios, larger β values are advantageous as they mitigate the smoothing effects of locally biased soft-labels; however, careful tuning is essential to avoid introducing biases that could negatively impact client model generalization.

V. LIMITATIONS AND FUTURE DIRECTIONS

While SCARLET represents a significant advancement in communication-efficient FL, several limitations merit further investigation to broaden its practical applicability. This section discusses these limitations and suggests directions for future research.

First, SCARLET, like other distillation-based FL approaches, depends on the availability of a shared public dataset whose distribution closely resembles, but does not necessarily match exactly, that of the clients' data. This dependency restricts the applicability scenarios for distillation-based FL methods. Knowledge distillation trains a student model to replicate the outputs of a teacher model for given inputs, essentially enforcing functional equivalence. In theory, even random noise could serve as the shared dataset; however, prior work demonstrates that this approach yields poor results [32]. Recent techniques leveraging generative models have been proposed to produce suitable synthetic data in place of a real public dataset [5], [33], [34]. Nevertheless, training generative models within an FL context still carries a risk of inadvertently exposing patterns of sensitive client data if not carefully managed. Thus, robust safeguards for privacypreserving synthetic data generation remain critical. Integrating these privacy-conscious data synthesis techniques offers a promising direction to broaden the practical applicability of distillation-based FL frameworks like SCARLET.

Second, the current implementation of SCARLET assumes a homogeneous model architecture across all clients and the server for analytical clarity and simplicity. However, one significant advantage of distillation-based FL is its inherent capability to support heterogeneous models. Several studies have demonstrated successful implementations of model heterogeneity within FL frameworks, covering both in clientserver model diversity [35] and inter-client variability [20]. Nevertheless, comprehensive evaluations of accuracy degradation resulting from introducing model heterogeneity remain limited, with only a handful of studies, such as [36] addressing this critical aspect. Consequently, the experimental validation of SCARLET and similar distillation-based FL frameworks under heterogeneous model conditions remains an open research area. Investigating this unexplored dimension is essential not only from an academic standpoint but also for practical FL deployments, where diverse device capabilities necessitate tailored model architectures across client devices.

Third, selecting hyperparameters for the soft-label caching mechanism, particularly the cache duration D, entails trade-

offs between reduced communication costs and model accuracy. While the current study employs a fixed cache duration, adaptive caching strategies—dynamically adjusting durations based on real-time performance metrics or selectively caching predictions—could further enhance communication efficiency and model performance under diverse FL conditions.

Finally, the Enhanced ERA mechanism presently relies on a static hyperparameter (β) to regulate aggregation sharpness. Given the inaccessibility of client-side data distributions, future research could explore dynamically adjusting β based on aggregated soft-label distributions or observed training dynamics. Such adaptive strategies would improve SCARLET's robustness and ability to manage varying degrees of data heterogeneity throughout FL.

In summary, future research directions include investigating synthetic data generation methods as alternatives to public datasets, evaluating SCARLET's efficacy in heterogeneous model settings, and developing adaptive caching strategies responsive to real-time performance metrics. Additionally, refining Enhanced ERA with adaptive aggregation sharpness mechanisms promises further improvements in handling diverse non-IID data scenarios.

VI. CONCLUSION

In this paper, we proposed SCARLET, a novel distillationbased FL framework that addresses key challenges in communication efficiency and data heterogeneity. By introducing the soft-label caching mechanism and the Enhanced ERA mechanism, SCARLET significantly reduces communication costs while maintaining competitive model accuracy. Extensive experiments demonstrated that SCARLET outperforms stateof-the-art distillation-based FL approaches in both server- and client-side evaluations. The modular design of SCARLET ensures compatibility with other FL frameworks, offering a flexible and scalable solution for diverse deployment scenarios. Despite its limitations, SCARLET represents a substantial step forward in communication-efficient FL. By further investigating adaptive caching strategies, model heterogeneity, and dynamic hyperparameter tuning, SCARLET could be extended to address a wider range of real-world challenges. This work lays the groundwork for future research, advancing the development of scalable, efficient, and robust FL frameworks.

ACKNOWLEDGMENTS

This work was supported by JST, PRESTO Grant Number JPMJPR2035, Japan, and was carried out using the TSUB-AME4.0 supercomputer at Institute of Science Tokyo.

APPENDIX A

PROOF OF MAJORIZATION FOR POWER EXPONENTS

In this Appendix, we present the mathematical proof of the majorization property introduced in Section III-D. Specifically, we prove that for any two power exponents β_1 and β_2 satisfying $\beta_2 > \beta_1 > 0$, the distribution produced by Enhanced ERA with exponent β_2 is majorized by the distribution produced with exponent β_1 . This result justifies the monotonic reduction

of entropy as β increases, leveraging the Schur-concavity of Shannon entropy.

Theorem 1 (Majorization via Power Exponents). Let $\{x_i\}_{i=1}^N$ be nonnegative real numbers in non-decreasing order,

$$0 \le x_1 \le x_2 \le \cdots \le x_N \le 1$$
,

and let

$$\sum_{i=1}^{N} x_i = 1.$$

For any $\beta_2 > \beta_1 > 0$, define the unnormalized vectors

$$X^{(\beta_1)} = (x_1^{\beta_1}, x_2^{\beta_1}, \dots, x_N^{\beta_1}),$$

$$X^{(\beta_2)} = (x_1^{\beta_2}, x_2^{\beta_2}, \dots, x_N^{\beta_2}),$$

and their corresponding normalized distributions

$$\hat{X}^{(\beta_1)} = \frac{X^{(\beta_1)}}{\sum_{j=1}^N x_j^{\beta_1}}, \qquad \hat{X}^{(\beta_2)} = \frac{X^{(\beta_2)}}{\sum_{j=1}^N x_j^{\beta_2}}.$$

Then, for each $1 \le k \le N$, the following holds:

$$\frac{\sum_{i=1}^{k} x_i^{\beta_2}}{\sum_{j=1}^{N} x_j^{\beta_2}} \le \frac{\sum_{i=1}^{k} x_i^{\beta_1}}{\sum_{j=1}^{N} x_j^{\beta_1}}.$$
 (5)

Equivalently, when viewed as probability distributions, $\hat{X}^{(\beta_2)}$ is *majorized* by $\hat{X}^{(\beta_1)}$.

Proof. Condition 1: Equality of Total Sums

Both normalized vectors sum to 1, satisfying the first requirement for majorization:

$$\sum_{i=1}^{N} \hat{X}_{i}^{(\beta_{1})} = 1 \quad \text{and} \quad \sum_{i=1}^{N} \hat{X}_{i}^{(\beta_{2})} = 1.$$

Condition 2: Prefix Sum Comparison

To prove the prefix sum dominance, we must show that for each $1 \le k \le N$,

$$\frac{\sum_{i=1}^k x_i^{\beta_2}}{\sum_{j=1}^N x_j^{\beta_2}} \le \frac{\sum_{i=1}^k x_i^{\beta_1}}{\sum_{j=1}^N x_j^{\beta_1}}.$$

a) Step 1: Power Function Properties

Since $0 \le x_i \le 1$ for all i and $\beta_2 > \beta_1 > 0$, raising x_i to the higher exponent β_2 decreases its value:

$$x_i^{\beta_2} = (x_i^{\beta_1})^{\frac{\beta_2}{\beta_1}} \le x_i^{\beta_1},$$

This inequality holds pointwise and extends to sums over subsets of indices:

$$\sum_{i=1}^{k} x_i^{\beta_2} \leq \sum_{i=1}^{k} x_i^{\beta_1}, \qquad \sum_{j=1}^{N} x_j^{\beta_2} \leq \sum_{i=1}^{N} x_j^{\beta_1}.$$

Method	Hyperparameter	Private Dataset CIFAR-10 CIFAR-100 Tiny ImageNet		
DS-FL	ERA temperature (T)	0.1	0.01	0.05
CFD	Upstream quantization bits $(b_{\rm up})$	1	1	1
	Downstream quantization bits $(b_{\rm down})$	32	32	32
COMET	Number of clusters (c)	2	2	3
	Regularization weight (λ)	1.0	1.0	1.0
Selective-FD	Client-side selector threshold (τ_{client})	0.0625	0.0625	0.03125
	Server-side selector threshold (τ_{server})	2.0	2.0	2.0

TABLE V: Method-Specific Hyperparameters for Each Private Dataset

b) Step 2: Ratio Comparison via Cross-Multiplication
To establish inequality 5, consider the cross-product inequality:

$$\left(\sum_{i=1}^k x_i^{\beta_2}\right) \left(\sum_{j=1}^N x_j^{\beta_1}\right) \leq \left(\sum_{i=1}^k x_i^{\beta_1}\right) \left(\sum_{j=1}^N x_j^{\beta_2}\right).$$

Rearranging this inequality confirms that the normalized prefix sums satisfy

$$\frac{\sum_{i=1}^{k} x_i^{\beta_2}}{\sum_{j=1}^{N} x_j^{\beta_2}} \le \frac{\sum_{i=1}^{k} x_i^{\beta_1}}{\sum_{j=1}^{N} x_j^{\beta_1}},$$

for all $1 \le k \le N$.

c) Conclusion

Both the normalization and prefix sum comparison conditions are satisfied, so $\hat{X}^{(\beta_2)}$ is majorized by $\hat{X}^{(\beta_1)}$. By the Schurconcavity of Shannon entropy, this implies that increasing the power exponent β reduces entropy, aligning with the statement in the main text.

This completes the proof.

APPENDIX B

HYPERPARAMETER SELECTION AND TUNING FOR COMPARATIVE ANALYSIS

To ensure the reproducibility of our experiments, we document the hyperparameter tuning process for each method and dataset in detail. The final hyperparameter values, summarized in Table V, were selected based on comprehensive testing across candidate configurations.

For DS-FL [3], the ERA temperature was tested over the range $T \in \{0.001, 0.005, 0.01, 0.05, 0.1, 0.5\}$. For CFD [4], based on insights from the original paper, we directly adopted the settings $b_{\rm up}=1$ and $b_{\rm down}=32$ without further tuning. For COMET [22], the number of clusters was tested within the range $c \in \{2,3,4\}$. Additionally, the regularization weight λ was tuned across $\lambda \in \{0.5,1.0,2.0\}$. For Selective-FD [23], the client-side selector threshold was adjusted with $\tau_{\rm client} \in \{0.03125, 0.0625, 0.125, 0.25\}$, and the server-side selector threshold was varied as $\tau_{\rm server} \in \{1.0, 1.5, 2.0\}$.

The selection of hyperparameters was guided by performance metrics tailored to each method. Specifically, for DS-FL and CFD, we prioritized server-side accuracy, choosing the configurations that achieved the highest accuracy on the server. In contrast, for COMET and Selective-FD, client-side performance was the primary criterion, and the configurations

yielding the highest client-side accuracy were selected. When multiple configurations exhibited similar accuracy, we opted for the one with faster convergence.

Certain methods required additional considerations. For Selective-FD, the official implementation does not include a server-side selector. We tested various values for the serverside selector threshold and found that $\tau_{\text{server}} = 2.0$, which effectively disables the selector, achieved the best accuracy. Consequently, our implementation for Selective-FD assumes no server-side selector. For CFD, delta coding was not included in our experiments (as no official implementation is available), as the original paper demonstrates that it primarily affects communication cost while having no impact on accuracy. With the upstream quantization already set to 1-bit in our setup, the absence of delta coding does not alter the accuracy results at all and only minimally affects the overall communication efficiency. For COMET, while the original paper focuses on soft-label aggregation without server-side model training, we extended the evaluation to include server-side training for consistency with other methods. This adjustment did not affect client-side evaluation. Furthermore, because COMET assumes partial client participation, we ensured fairness by determining client cluster assignments server-side and transmitting this information directly to each client, thereby avoiding additional communication costs from clustering.

These considerations ensure that each method is fairly evaluated under consistent conditions, taking into account their unique characteristics and theoretical assumptions. The final configurations adopted for each private dataset setting are detailed in Table V.

REFERENCES

- [1] B. McMahan, E. Moore, D. Ramage, S. Hampson, and B. A. y. Arcas, "Communication-Efficient Learning of Deep Networks from Decentralized Data," in *Proc. 20th Int. Conf. Artif. Intell. Stat.*, ser. Proc. Mach. Learn. Res., A. Singh and J. Zhu, Eds., vol. 54. PMLR, 2017, pp. 1273–1282.
- [2] T. Li, A. K. Sahu, A. Talwalkar, and V. Smith, "Federated Learning: Challenges, Methods, and Future Directions," *IEEE Signal Process. Mag.*, vol. 37, no. 3, pp. 50–60, 2020.
- [3] S. Itahara, T. Nishio, Y. Koda, M. Morikura, and K. Yamamoto, "Distillation-Based Semi-Supervised Federated Learning for Communication-Efficient Collaborative Training With Non-IID Private Data," *IEEE Trans. Mobile Comput.*, vol. 22, no. 1, pp. 191–205, 2023.
- [4] F. Sattler, A. Marban, R. Rischke, and W. Samek, "CFD: Communication-Efficient Federated Distillation via Soft-Label Quantization and Delta Coding," *IEEE Trans. Netw. Sci. Eng.*, vol. 9, no. 4, pp. 2025–2038, 2022.

- [5] Z. Zhu, J. Hong, and J. Zhou, "Data-Free Knowledge Distillation for Heterogeneous Federated Learning," in *Proc. 38th Int. Conf. Mach. Learn. (ICML)*, ser. Proc. Mach. Learn. Res., M. Meila and T. Zhang, Eds., vol. 139. PMLR, 2021, pp. 12878–12889.
- [6] J. Zhang, S. Guo, X. Ma, H. Wang, W. Xu, and F. Wu, "Parameterized Knowledge Transfer for Personalized Federated Learning," Adv. Neural Inf. Process. Syst. (NeurIPS), vol. 34, pp. 10092–10104, 2021.
- [7] C. Wang, G. Yang, G. Papanastasiou, H. Zhang, J. J. P. C. Rodrigues, and V. H. C. de Albuquerque, "Industrial Cyber-Physical Systems-Based Cloud IoT Edge for Federated Heterogeneous Distillation," *IEEE Trans. Ind. Informat.*, vol. 17, no. 8, pp. 5511–5521, 2021.
- [8] X. Gong, A. Sharma, S. Karanam, Z. Wu, T. Chen, D. Doermann, and A. Innanje, "Ensemble Attention Distillation for Privacy-Preserving Federated LearningEnsemble Attention Distillation for Privacy-Preserving Federated Learning," in *Proc. IEEE/CVF Int. Conf. Comput. Vis. (ICCV)*, 2021, pp. 15056–15066.
- [9] —, "Preserving Privacy in Federated Learning with Ensemble Cross-Domain Knowledge Distillation," in *Proc. AAAI Conf. Artif. Intell.*, vol. 36, no. 11, 2022, pp. 11 891–11 899.
- [10] C. T. Dinh, N. Tran, and J. Nguyen, "Personalized Federated Learning with Moreau Envelopes," in *Proc. Adv. Neural Inf. Process. Syst.*, H. Larochelle, M. Ranzato, R. Hadsell, M. Balcan, and H. Lin, Eds., vol. 33. Curran Associates, Inc., 2020, pp. 21394–21405.
- [11] T. Li, A. K. Sahu, M. Zaheer, M. Sanjabi, A. Talwalkar, and V. Smith, "Federated Optimization in Heterogeneous Networks," in *Proc. Mach. Learn. Syst.*, I. Dhillon, D. Papailiopoulos, and V. Sze, Eds., vol. 2, 2020, pp. 429–450.
- [12] S. P. Karimireddy, S. Kale, M. Mohri, S. Reddi, S. Stich, and A. T. Suresh, "SCAFFOLD: Stochastic Controlled Averaging for Federated Learning," in *Proc. 37th Int. Conf. Mach. Learn.*, ser. Proc. Mach. Learn. Res., H. D. III and A. Singh, Eds., vol. 119. PMLR, 2020, pp. 5132–5143.
- [13] G. Lee, M. Jeong, Y. Shin, S. Bae, and S.-Y. Yun, "Preservation of the Global Knowledge by Not-True Distillation in Federated Learning," in *Proc. Adv. Neural Inf. Process. Syst.*, S. Koyejo, S. Mohamed, A. Agarwal, D. Belgrave, K. Cho, and A. Oh, Eds., vol. 35. Curran Associates, Inc., 2022, pp. 38 461–38 474.
- [14] A. Reisizadeh, A. Mokhtari, H. Hassani, A. Jadbabaie, and R. Pedarsani, "FedPAQ: A Communication-Efficient Federated Learning Method with Periodic Averaging and Quantization," in *Proc. 23rd Int. Conf. Artif. Intell. Stat.*, ser. Proc. Mach. Learn. Res., S. Chiappa and R. Calandra, Eds., vol. 108. PMLR, 2020, pp. 2021–2031.
- [15] F. Haddadpour, M. M. Kamani, A. Mokhtari, and M. Mahdavi, "Federated Learning with Compression: Unified Analysis and Sharp Guarantees," in *Proc. 24th Int. Conf. Artif. Intell. Stat.*, ser. Proc. Mach. Learn. Res., A. Banerjee and K. Fukumizu, Eds., vol. 130. PMLR, 13–15 Apr 2021, pp. 2350–2358.
- [16] P. Han, S. Wang, and K. K. Leung, "Adaptive Gradient Sparsification for Efficient Federated Learning: An Online Learning Approach," in Proc. 40th IEEE Int. Conf. Distrib. Comput. Syst. (ICDCS), 2020, pp. 300–310.
- [17] T. Lin, L. Kong, S. U. Stich, and M. Jaggi, "Ensemble Distillation for Robust Model Fusion in Federated Learning," in *Proc. Adv. Neural Inf. Process. Syst.*, H. Larochelle, M. Ranzato, R. Hadsell, M. Balcan, and H. Lin, Eds., vol. 33. Curran Associates, Inc., 2020, pp. 2351–2363.
- [18] C. Wu, F. Wu, L. Lyu, Y. Huang, and X. Xie, "Communication-Efficient Federated Learning via Knowledge Distillation," *Nature Commun.*, vol. 13, no. 1, p. 2032, 2022.
- [19] G. Hinton, O. Vinyals, and J. Dean, "Distilling the Knowledge in a Neural Network," in NIPS Deep Learn. Represent. Learn. Workshop, 2015.
- [20] D. Li and J. Wang, "FedMD: Heterogenous Federated Learning via Model Distillation," arXiv:1910.03581, 2019.
- [21] E. Jeong, S. Oh, H. Kim, J. Park, M. Bennis, and S.-L. Kim, "Communication-Efficient On-Device Machine Learning: Federated Distillation and Augmentation under Non-IID Private Data," in *NeurIPS Workshop on Mach. Learn. Phone Consum. Devices (MLPCD)*, 2018.
- [22] Y. J. Cho, J. Wang, T. Chirvolu, and G. Joshi, "Communication-Efficient and Model-Heterogeneous Personalized Federated Learning via Clustered Knowledge Transfer," *IEEE J. Sel. Top. Signal Process.*, vol. 17, no. 1, pp. 234–247, 2023.
- [23] J. Shao, F. Wu, and J. Zhang, "Selective knowledge sharing for privacy-preserving federated distillation without a good teacher," *Nature Commun.*, vol. 15, no. 1, p. 349, 2024.
- [24] Y. Liu, L. Su, C. Joe-Wong, S. Ioannidis, E. Yeh, and M. Siew, "Cache-Enabled Federated Learning Systems," in *Proc. 24th Int. Symp. Theory*,

- Algorithmic Foundations, and Protocol Design for Mobile Netw. and Mobile Comput., 2023, pp. 1–11.
- [25] Z. Wu, S. Sun, Y. Wang, M. Liu, K. Xu, W. Wang, X. Jiang, B. Gao, and J. Lu, "FedCache: A Knowledge Cache-Driven Federated Learning Architecture for Personalized Edge Intelligence," *IEEE Trans. Mobile Comput.*, vol. 23, no. 10, pp. 9368–9382, 2024.
- [26] Q. Pan, S. Sun, Z. Wu, Y. Wang, M. Liu, and B. Gao, "FedCache 2.0: Exploiting the Potential of Distilled Data in Knowledge Cache-driven Federated Learning," arXiv:2405.13378, 2024.
- [27] A. Krizhevsky, G. Hinton et al., "Learning Multiple Layers of Features from Tiny Images," 2009.
- [28] Y. Le and X. Yang, "Tiny ImageNet Visual Recognition Challenge," CS 231N, vol. 7, no. 7, p. 3, 2015.
- [29] G. Griffin, A. Holub, P. Perona et al., "Caltech-256 Object Category Dataset," California Inst. Technol. Pasadena, Tech. Rep. 7694, 2007.
- [30] T.-M. H. Hsu, H. Qi, and M. Brown, "Measuring the Effects of Non-Identical Data Distribution for Federated Visual Classification," arXiv:1909.06335, 2019.
- [31] K. He, X. Zhang, S. Ren, and J. Sun, "Deep Residual Learning for Image Recognition," in *Proc. IEEE Conf. Comput. Vis. Pattern Recognit.* (CVPR), 2016, pp. 770–778.
- [32] S. Stanton, P. Izmailov, P. Kirichenko, A. A. Alemi, and A. G. Wilson, "Does Knowledge Distillation Really Work?" Adv. Neural Inf. Process. Syst. (NeurIPS), vol. 34, pp. 6906–6919, 2021.
- [33] Y. Wu, Y. Kang, J. Luo, Y. He, L. Fan, R. Pan, and Q. Yang, "Fedcg: Leverage conditional gan for protecting privacy and maintaining competitive performance in federated learning," in *Proc. 31st Int. Joint Conf. Artif. Intell. (IJCAI)*, L. D. Raedt, Ed. Int. Joint Conf. Artif. Intell. Org., 2022, pp. 2334–2340.
- [34] X. Gong, S. Li, Y. Bao, B. Yao, Y. Huang, Z. Wu, B. Zhang, Y. Zheng, and D. Doermann, "Federated learning via input-output collaborative distillation," in *Proc. AAAI Conf. Artif. Intell.*, vol. 38, no. 20, 2024, pp. 22 058–22 066.
- [35] C. He, M. Annavaram, and S. Avestimehr, "Group Knowledge Transfer: Federated Learning of Large CNNs at the Edge," Adv. Neural Inf. Process. Syst. (NeurIPS), vol. 33, pp. 14068–14080, 2020.
- [36] A. Taya, T. Nishio, M. Morikura, and K. Yamamoto, "Decentralized and model-free federated learning: Consensus-based distillation in function space," *IEEE Trans. Signal Inf. Process. Netw.*, vol. 8, pp. 799–814, 2022.